Equivalent-particle approximations in electron and photon processes of higher-order QED*

Min-Shih Chen

*Stanford Linear Accelerator Center, Stanford, California 94305
and Physics Department, University of Michigan, Ann Arbor, Michigan 48104* [†]

Peter Zerwas[‡]

Stanford Linear Accelerator Center, Stanford, California 94305
(Received 6 March 1975)

The method of equivalent-photon and -lepton approximations is applied to speedy estimates of higher-order QED cross sections in high-energy electron-positron annihilation and inelastic photon- and electron-nucleon scattering. The equivalent-particle spectra are derived with infinite-momentum-frame techniques. The limitations of the approximation scheme are discussed thoroughly.

I. INTRODUCTION

The equivalent-photon approximation was first developed by von Weizsäcker and Williams[1] in 1934. It is a very useful instrument for calculating complicated cross sections in small-angle electron scattering. For high-energy electrons, these cross sections can be written as a convolution of the probability that the electron radiates off a photon, with the corresponding photon cross section. A similar approximation should work for related processes, such as photon bremsstrahlung and photon splitting into electron-positron pairs, as well. All these examples have in common that a light or zero-mass particle splits into a pair of light or zero-mass particles. The constituents of this daughter pair subsequently react (as equivalent beams) with the target system in a subprocess which is easier to describe than the original reaction [see Figs. 1(a)–1(c)]. The extension to photon bremsstrahlung and photon splitting was first done by Kessler[2] and has recently been discussed by Baier, Fadin, and Khoze.[3]

The main purpose of our article is the application of the equivalent-photon and -lepton method to derive simple, approximate expressions for cross sections of radiation processes which frequently occur in lepton-lepton collisions and electron- or photon-nucleon scattering. Among those are bremsstrahlung corrections in electron-positron annihilation and inelastic electron-nucleon scattering (spin analysis included). In addition, we derive a simple formula for pair production in photon-nucleon scattering. Some of the results can already be found in the literature. However, we shall repeat material where necessary because we want to present a coherent picture of the processes under discussion. Besides those phenomenological applications, we briefly derive the equivalent-photon and -lepton spectra with the infinite-momentum technique[4] which provides the most powerful method for tree-graph calculations in high-energy quantum electrodynamics. We repeat the derivation of the spectra with this method[5] in order to enlighten the approximations involved, which forbid a blind use of the approach. In addition, we shall compare the results obtained by the equivalent-particle method with exact calculations of simple examples in order to provide the reader with an estimate of the degree of accuracy of our formulas when applied to everyday experimental problems.

Our paper is organized as follows. In Sec. II we give a brief derivation of the equivalent-photon and -lepton spectra in the infinite-momentum frame and discuss the approximations underlying this approach. In Sec. III, we describe simple applications to electron-positron annihilation and inelastic electron-nucleon scattering and compare the approximate results with exact calculations. Section IV contains some multistep applications, in which the equivalent photons and leptons themselves are again parents of other equivalent photons and leptons. Finally, in Sec. V we summarize the results and add some general comments.
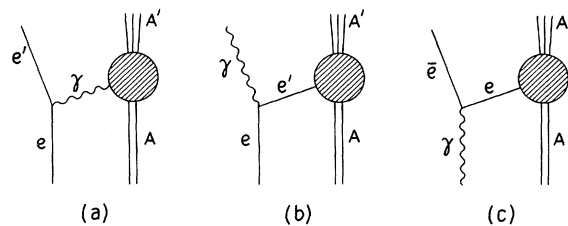

FIG. 1. Equivalent-particle approximation in electron and photon scattering.

II. EQUIVALENT-PHOTON AND -LEPTON SPECTRA

The derivation of the equivalent-photon and -lepton spectra is well known.[1-3,5] Nevertheless, we shall give a short derivation of the Weizsäcker-Williams formula using the technique of the time-ordered perturbation theory in the infinite-momentum frame.[4] In the same way, we sketch the derivation of the lepton spectra as well. That is done in order to examine all the approximations involved in the final formulas which set certain limits to their applicability.

First, we consider (inelastic) electron scattering on a target A, $e + A \rightarrow e' + A'$, in the single-photon approximation, as illustrated in Fig. 2. In time-ordered perturbation theory, the transition amplitude is given by

$$T_{fi} = \sum_n \frac{\langle f|H|n\rangle \langle n|H|i\rangle}{E_i - E_n} , \tag{1}$$

where the sum is to be performed over all intermediate states $|n\rangle$ corresponding to lines in Fig. 2 which are cut; H is the interaction Hamiltonian,
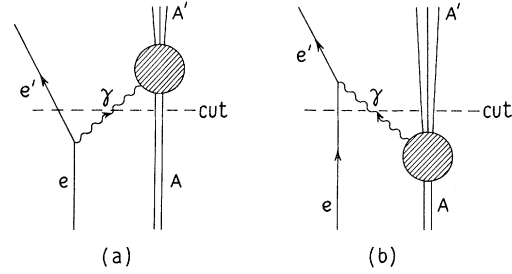

FIG. 2. One-photon exchange diagrams contributing to electron scattering on a target A in time-ordered perturbation theory.

and E_i and E_n are the initial and intermediate energies, respectively. In this approach, vertices do not conserve energy but only momentum. We first calculate the contribution from Fig. 2(a), where the electron emits a photon which is subsequently absorbed by the (A, A') system. Thus, with $|n\rangle = |e', \gamma(\lambda), A\rangle$ the T matrix in Eq. (1) can be written as

$$T(eA \rightarrow e'A') = e \sum_{\lambda = \pm} \frac{\bar{u}(e') \, \slashed{\epsilon}(\lambda) \, u(e) \langle A'|H|\gamma(\lambda), A\rangle}{2E(\gamma)[E(e) - E(e') - E(\gamma)]} \Bigg|_{\vec{p}(\gamma) = \vec{p}(e) - \vec{p}(e')} + \cdots . \tag{2}$$

The remaining sum runs over the longitudinal and scalar polarizations of the intermediate photon. All expressions have a particularly simple form in the infinite momentum frame ($p \rightarrow \infty$) where the momenta can be parameterized as

$$p(e) = \left\{ P + \frac{1}{2} \frac{m_e^2}{P} , \vec{0}, P \right\} , \tag{3a}$$

$$p(e') = \left\{ (1 - x) P + \frac{1}{2} \frac{m_e^2 + \vec{p}_\perp^2}{(1 - x)P} , \vec{p}_\perp, (1 - x)P \right\} , \tag{3b}$$

$$p(\gamma) = \left\{ xP + \frac{1}{2} \frac{\vec{p}_\perp^2}{xP} , -\vec{p}_\perp, xP \right\} . \tag{3c}$$

The denominator in Eq. (2) turns out to be $-(\vec{p}_\perp^2 + m_e^2 x^2)/(1 - x)$. Hence, most of the contributions to the cross section come from the small-$\vec{p}_\perp$ region where the inverse electron mass determines the scale of the T matrix. As a consequence, the contribution from diagram 2(b) is much smaller and can be neglected as long as one of the invariant A or A' masses is much larger than the electron mass. The square of the numerator, on the other hand, can be simplified by observing that

$$\sum_{\text{el spins}} [\bar{u}(e') \slashed{\epsilon}(\lambda') u(e)]^* [\bar{u}(e') \slashed{\epsilon}(\lambda) u(e)] = \delta_{\lambda\lambda'} \frac{2\vec{p}_\perp^2}{x^2(1 - x)} [1 + (1 - x)^2] + \cdots . \tag{4}$$

Terms which vanish if the transverse momenta of the final electron are averaged, have been discarded. Longitudinal and scalar polarizations do not contribute in the leading order of $\vec{p}_\perp^2$. So, the square of the T matrix can be written as

$$\sum_{\text{el spins}} |T(eA \rightarrow e'A')|^2 = e^2 \frac{2(1 - x)}{x^2(\vec{p}_\perp^2 + m_e^2 x^2)} [1 + (1 - x)^2] \sum_\lambda |T(\gamma(\lambda)A \rightarrow A')|^2 . \tag{5}$$

Integrating over all electron momenta in the final state and taking the correct flux factors into account, we get the following result for the cross section:

$$\sigma(eA \rightarrow e'A') = \frac{\alpha}{\pi} \int_0^1 dx \, \frac{1+(1-x)^2}{x} \, \ln \frac{p_\perp^{max}}{m_e x} \, \sigma(\gamma A \rightarrow A') \bigg|_{E(\gamma) = xE(e)} \tag{6}$$

The transverse momentum cutoff $p_\perp^{max}$ is invariant under Lorentz boosts along the direction of the incident electron, and it can be expressed in terms of energy and scattering angle of the electron in the laboratory frame as

$$p_\perp^{max} \simeq E(e') \, \theta^{max} \simeq (1-x) \, E \theta^{max} \quad . \tag{7}$$

For many applications at presently available energies, one can neglect the logarithmic x and θ dependence. Then the equivalent-photon spectrum in Eq. (6) is given by

$$F_e^\gamma(E, x) = \frac{\alpha}{\pi} \ln \frac{E}{m_e} \, \frac{1+(1-x)^2}{x} \,, \tag{8}$$

where x denotes the fraction of the incident electron energy which is carried away by the photon. Thus, electron scattering cross sections can be expressed by a simple convolution of the equivalent photon spectrum $F_e^\gamma(E, x)$ with the corresponding photon cross section:

$$\sigma(e(E) + A \rightarrow e' + A') = \int_0^1 dx \, F_e^\gamma(E, x) \, \sigma(\gamma(xE) + A \rightarrow A') \quad . \tag{9}$$

The equivalent-lepton spectra can be found in the same fashion. The probability that an electron with energy E radiates off a photon and transforms into an electron with energy xE is simply given by Eq. (9) with x replaced by $(1-x)$ [see Fig. 1(b)]:

$$F_e^e(E, x) = \frac{\alpha}{\pi} \ln \frac{E}{m_e} \, \frac{1+x^2}{1-x} \,. \tag{10}$$

To derive the electron content of the photon [Fig. 1(c)], we can proceed analogously. While the kinematics is the same in all three cases under discussion, we find the square of the current matrix element for photon splitting by a simple crossing trick. Writing the right-hand side of Eq. (4) in the symmetric form

$$2\left[\frac{\vec{p}_\perp^2}{xP} + \frac{\vec{p}_\perp^2}{(1-x)P} \right] \frac{P^2 + (1-x)^2 P^2}{xP} \,,$$

we obtain the corresponding expression for photon splitting by exchanging the photon and electron momenta,

$$xP \rightleftharpoons P \text{ and } (1-x) \, P \rightleftharpoons (1-x)P \,,$$

but leaving the parenthesis unchanged (since the expression is already symmetric in the new electron and positron variables). Thus the equivalent electron spectrum of the photon is given by

$$F_\gamma^e(E, x) = \frac{\alpha}{\pi} \ln \frac{E}{m_e} [x^2 + (1-x)^2] \quad . \tag{11}$$

The photon splitting spectrum does not develop the infrared pole at $x \rightarrow 0$, in contrast to the previously derived photon radiation spectra. The spin dependence can easily be analyzed by observing that the electromagnetic vertex conserves helicity for fast leptons.

We summarize the results obtained so far in Fig. 3. The daughter particle which scatters on the target is marked by a little cross.

An amusing question concerns the metamorphosis of an electron into a positron. This probability can be found by radiating off the electron a photon which subsequently splits into an electron-positron pair (see Fig. 4):

$$\sigma(e(E) + A \rightarrow A' + \cdots)$$

$$= \int_0^1 dx \, F_e^\gamma(E, x) \int_0^1 F_\gamma^e(xE, y) \, \sigma(\bar{e}(xyE) + A \rightarrow A')$$

$$\equiv \int_0^1 dz \, {}_2F_e^e(E, z) \, \sigma(\bar{e}(zE) + A \rightarrow A') \,, \tag{12}$$

SYMBOL	SPECTRUM
	$F_e^\gamma(E,x) = \frac{\alpha}{\pi}\left(\ln\frac{E}{m_e}\right)\frac{1+(1-x)^2}{x}$
	$F_e^e(E,x) = \frac{\alpha}{\pi}\left(\ln\frac{E}{m_e}\right)\frac{1+x^2}{1-x}$
	$F_\gamma^e(E,x) = \frac{\alpha}{\pi}\left(\ln\frac{E}{m_e}\right)\left[x^2+(1-x)^2\right]$
	$F_{e(\lambda)}^{e'(\lambda')}(E,x) = \delta_{\lambda\lambda'}\frac{\alpha}{\pi}\left(\ln\frac{E}{m_e}\right)\frac{1+x^2}{1-x}$

FIG. 3. Single-step equivalent-particle spectra. The daughter particle which scatters on the target is marked by a cross.
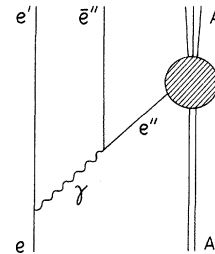

FIG. 4. Double-step equivalent-photon/electron approximation.

with

$$_2F_e^e(E, z) = \int_z^1 \frac{dx}{x} F_e^\gamma(E, x) F_\gamma^e\left(xE, \frac{z}{x}\right) \qquad (13)$$

$$\simeq 2\left(\frac{\alpha}{\pi}\right)^2 \ln\frac{E}{m_e}\left(\frac{1}{z}\ln\frac{zE}{m_e} - \ln\frac{E}{m_e}\right). \qquad (13')$$

In the same way, one obtains the secondary photon distribution within a photon:

$$_2F_\gamma^\gamma(E, z) = 2\int_z^1 \frac{dx}{x} F_\gamma^e(E, x) F_e^\gamma\left(xE, \frac{z}{x}\right) \qquad (14)$$

$$\simeq 4\left(\frac{\alpha}{\pi}\right)^2 \ln\frac{E}{m_e}\left(\frac{1}{z}\ln\frac{E}{m_e} - \ln\frac{zE}{m_e}\right). \qquad (14')$$

The factor of 2 appears because the final-state photon can be radiated off the electron and the positron produced in the first step.

We do not want to elaborate these two-step formulas in detail because they can be used only for rough estimates. Instead, we neglect all x-dependent numerators in the expressions of Fig. 3 and obtain in this way approximate two-step spectra. The results are presented in Fig. 5.

It is easy to see that the differences between the first three rows of Fig. 5 and those of Fig. 3 are bounded within a factor of 2. The accuracy of the double-step expressions in the last two rows of Fig. 5 is no worse than a factor of 4 relative to Eqs. (13') and (14'), as long as the equivalent particles are not near their kinematical limits (with $x \simeq 1$). For $x \simeq 1$, only Eqs. (13') and (14') can give the correct threshold behavior. The simplicity
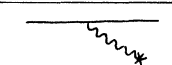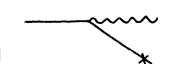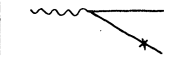
of the expressions in Fig. 5 compensates for their lack of accuracy.

We should like to complete this section by summarizing briefly the main ingredients in deriving the equivalent-photon and -lepton spectra and, as a consequence, by giving some words of caution which should prevent the reader from a wrong use of the formulas:

(i) At least one of the A and A' masses must be heavy enough not to induce substantial bremsstrahlung effects; otherwise, we cannot neglect diagrams in which the intermediate photon or lepton is absorbed by the incident lepton or photon projectile. That does not contradict the use of double Weizsäcker-Williams spectra for processes such as $ee \to eeX$, in which case the subprocess $\gamma + e(\equiv A) \to e' + X(\equiv A')$ itself is again resolved by the equivalent-photon method.

(ii) The azimuth angles of the emitted particle have been averaged. Therefore, one can apply this form of the equivalent-particle approximation only to processes in which the absorption of the equivalent particle by the target is insensitive to little changes of the transverse momenta. Furthermore, measuring the transition $A \to A'$ must not constrain the angle of the emitted photon or lepton, but must leave the particle with enough kinematical degrees of freedom.

(iii) Only the leading logarithm in $p_\perp^{max}$ is gauge invariant and one has to employ more refined formulas if a *minimum* transverse-momentum cutoff is experimentally enforced.

(iv) The spectra without angular dependence[6] can only be applied to cases where the maximum scattering angle in the laboratory frame is not yet too severely restricted to extremely small values by $\theta^{max} \propto E^{-1/2}$.

III. ONE-STEP APPLICATIONS

Most of the applications of the equivalent-photon approximation have been described in excellent review articles.[7] Therefore, we concentrate in this section on simple examples of the equivalent-electron approximation and compare the results with covariant Feynman-diagram calculations.

A. $e^+e^- \to \gamma f$ (hard-photon bremsstrahlung)

This bremsstrahlung process[3] is shown in Fig. 6(a). It can serve as an instrument to study the low-energy behavior of the e^+e^- annihilation because the hard photon can carry away a large portion of the initial energy. Denoting by $(1 - x)$ the fraction of energy the photon snatches away from the incident lepton, the invariant mass M of the final state f reads

SYMBOL	SPECTRUM
	$F_e^\gamma(E, x) \simeq \frac{2\alpha}{\pi}\left(\ln\frac{E}{m_e}\right)\frac{1}{x}$
	$F_e^e(E, x) \simeq \frac{2\alpha}{\pi}\left(\ln\frac{E}{m_e}\right)\frac{1}{1-x}$
	$F_\gamma^e(E, x) \simeq \frac{\alpha}{\pi}\left(\ln\frac{E}{m_e}\right)\frac{1}{x}$
	$_2F_e^e(E, x) \simeq 2\left(\frac{\alpha}{\pi}\ln\frac{E}{m_e}\right)^2 \frac{1}{x}$
	$_2F_\gamma^\gamma(E, x) \simeq 4\left(\frac{\alpha}{\pi}\ln\frac{E}{m_e}\right)^2 \frac{1}{x}$

FIG. 5. Approximate single- and double-step equivalent-particle spectra. The daughter particle which scatters on the target is marked by a cross.

$$M^2 = 4xE^2 \tag{15}$$

($2E$ is the invariant energy of the e^+e^- system). Thus, from $d\sigma/dx = F_e^e \sigma_f$, with F_e^e taken from Fig. 3, we obtain the result

$$\frac{d\sigma}{dM^2} = \frac{2\alpha}{\pi} \ln \frac{E}{m_e} \frac{1}{4E^2} \frac{1+(M^2/4E^2)^2}{1-(M^2/4E^2)} \sigma_{e^+e^- \to f}(M^2) , \tag{16}$$

which agrees with the small-angle limit of the covariant and gauge-invariant calculation in Ref. 8.

B. $e\gamma \to \mu^+\mu^-$ (electron scattered into forward hemisphere)

This process corresponds to muon pair production in inelastic electron scattering off a photon target [Fig. 6(b)]. Replacing the muons by a light quark-antiquark pair, we can use the cross section as an estimate for deep-inelastic electron-photon scattering.

What we need to calculate the high-energy limit of this cross section, is the muon-pair wave function of the photon (see Fig. 3, with $m_e \to m_\mu$) and the elastic electron-muon scattering cross section. For our special purpose, we write the latter in the following form, which is somewhat unusual, but is familiar to every parton theorist:

$$\frac{d\sigma^{\mu e}}{dQ^2} = \frac{4\pi\alpha^2}{Q^4} \left(1 - y + \frac{y^2}{2} \right) , \tag{17}$$

where $(-Q^2)$ is the invariant momentum transfer at the electron-photon vertex and y is the energy loss in the muon rest frame:

$$y = \frac{p(\mu) \cdot [p(e) - p(e')]}{p(\mu) \cdot p(e)} . \tag{18}$$

Notice that y is scale invariant under $p(\mu) \to xp(\mu)$. In analogy to electron-nucleon scattering one introduces the variables

$$\nu = p(\gamma) \cdot [p(e) - p(e')] , \tag{19a}$$

$$x = Q^2/2\nu . \tag{19b}$$

With $p(\mu) = x'p(\gamma)$, the Rutherford formula can formally be written as

$$\frac{d^2\sigma^{\mu e}}{dQ^2 d\nu} = \frac{4\pi\alpha^2}{Q^4} \left(1 - y + \frac{y^2}{2} \right) x'\delta\left(x'\nu - \frac{Q^2}{2} \right). \tag{20}$$

In this form it can easily be folded with the equivalent-muon spectrum:

$$\frac{d^2\sigma}{dQ^2 d\nu} = 2\int_0^1 dx' F_\gamma^\mu(E, x') \frac{d^2\sigma^{\mu e}}{dQ^2 d\nu} . \tag{21}$$

(The factor of 2 comes from coupling the heavy photon to both μ^+ and μ^-.) Then,

$$\frac{d^2\sigma}{dQ^2 dx} = \frac{8\alpha^3}{Q^4} [x^2 + (1-x)^2] \left(1 - y + \frac{y^2}{2} \right) \ln \frac{E}{m_\mu} . \tag{22}$$

This result is identical with Fujikawa's covariant treatment of this process,[9] apart from the argument of the logarithm which is to be replaced by the invariant $(\mu^+\mu^-)$ pair mass, $W(\mu^+\mu^-)$. However $W(\mu^+\mu^-)$ and E are logarithmically equivalent, as long as we are in the *Bjorken limit* with x and y being finite for finite scattering angles.

C. $e\gamma \to e'f$ (electron scattered into backward hemisphere)

For backward-scattered electrons, the diagram drawn in Fig. 6(c) is dominant. For a given value of $M^2 = P^2(f)$ we have

$$M^2 = 4xE_\gamma E , \tag{23}$$

where E_γ and E are the energies of the incident photon and electron, respectively. In the equivalent-electron approximation, the cross section can be written as

$$\frac{d\sigma}{dM^2} = \frac{1}{4xE^2} F_\gamma^e(E_\gamma, x) \sigma_{e^+e^- \to f}(M^2)$$

$$= \frac{\alpha}{2\pi} \frac{\sigma_{e^+e^- \to f}(M^2)}{4EE_\gamma} \left[1 + \left(1 - \frac{M^2}{4E^2} \right)^2 \right] \ln \frac{E_\gamma}{m_e} . \tag{24}$$

This result is again logarithmically equivalent to the covariant approach[8] as long as all energies involved, as well as the mass M, are of comparable magnitude (generalized Bjorken limit).
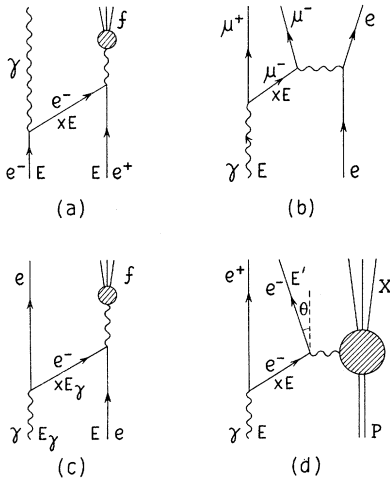

FIG. 6. (a) Hard-photon bremsstrahlung in electron-positron collisions; (b) inelastic electron-photon scattering with forward-scattered electron; (c) inelastic electron Compton scattering with backward-scattered electrons; (d) pair production in photon-proton scattering.

D. Bethe-Heitler pair production in $\gamma p \to e^+ e^- X$

Bethe-Heitler pair production[10] is an important background to the direct production of positron-electron of V pairs within the proton. As seen from Fig. 6(d), the cross section can be written

$$\frac{d^2\sigma}{dE' \, d\Omega'} = \frac{\alpha}{\pi} \ln \frac{E}{m_e} \int_{x_0}^{1} dx \, [1 + (1-x)^2] \left[\frac{d^2\sigma(ep \to e'X)}{dE' \, d\Omega'} \right]_{E(e) = xE} . \tag{25}$$

The lower limit x_0 is determined by the elastic transition at the hadron-vertex (m_p denotes the nucleon mass):

$$x_0 = \frac{m_p E'}{m_p E - 2EE' \sin^2(\frac{1}{2}\theta')} . \tag{26}$$

In terms of the familiar structure functions $W_{1,2}(\nu, Q^2)$ this result reads

$$\frac{d^2\sigma}{dE' \, d\Omega'} = \frac{\alpha^2}{4E^2 \sin^2(\frac{1}{2}\theta)} \left[W_2^\gamma(E, E', \theta') \cos^2(\frac{1}{2}\theta') + 2 W_1^\gamma(E, E', \theta) \sin^2(\frac{1}{2}\theta') \right] , \tag{27}$$

with

$$W_{1,2}^\gamma(E, E', \theta') = \frac{\alpha}{\pi} \ln \frac{E}{m_e} \int_{x_0}^{1} \frac{dx \, [x^2 + (1-x)^2]}{x^2} W_{1,2}(xE - E', 4xEE') \sin^2(\frac{1}{2}\theta'). \tag{28}$$

To evaluate these integrals one must know the structure functions on the ray

$$Q^2 = 4(\nu + E') E' \sin^2(\frac{1}{2}\theta') \tag{29}$$

in the (ν, Q^2) plane. Instead of going into details, we consider the approximation where the target is very heavy and pointlike.[2] Then

$$W_1 = W_2 = \delta_1(xE - E') , \tag{30}$$

and the cross section reads for *finite values of* θ' *and* E'

$$\frac{d^2\sigma}{dE' \, d\Omega'} = \frac{\alpha^3}{4\pi} \frac{1 + \sin^2(\frac{1}{2}\theta')}{\sin^4(\frac{1}{2}\theta')} \frac{E'^2 + (E - E')^2}{E'^2 E^3} \ln \frac{E}{m_e} . \tag{31}$$

E. Application to radiative corrections

Radiative corrections are particularly important in leptonic and semileptonic processes. Although a precise evaluation requires a very careful treatment,[10] the equivalent-photon and -lepton approximation provides a simple tool for a speedy estimate. Let us consider electron scattering on a target via one-photon exchange, as illustrated in Fig. 7(a). The radiative corrections in the lowest order of α are the last three terms. The second term, together with the infrared part of the last two terms, contributes to the electron-photon vertex correction. This part is independent of the target, and the analytical result can be found in the literature. The real "hard"-photon emissions from the last two terms are target-dependent and have to be evaluated for each reaction separately.

in terms of the cross section for electron scattering off the proton. If the positron is scattered with small angle but the electron with fairly large angle, then the differential cross section is given in the lab frame by

1. Deep-inelastic electron-proton scattering

As is well known, this process can be described in terms of two kinematical variables Q^2 and ν,

$$Q^2 = -(p - p')^2 \quad \text{and} \quad \nu = (p - p') \cdot P/m_p , \tag{32}$$

where p, p', and P are defined as in Fig. 7(a). The most important contribution to the cross section

$$f(\nu, Q^2) \equiv \frac{d^2\sigma}{d\nu \, dQ^2} \tag{33}$$

is the single-photon exchange term $f^{(0)}(\nu, Q^2)$, which can be expressed in terms of the well-known proton structure functions. The contributions from the last two terms in Fig. 7(a) are the radiative corrections from real photon emission and can be written as a convolution of the equivalent-lepton spectrum with $f^{(0)}(\nu, Q^2)$. The process shown as the third term in the figure can be interpreted in the following fashion: The incident electron emits a photon of momentum $(1 - x)p$ and the equivalent electron of momentum xp scatters off the target by one photon exchange. In the equivalent electron-proton scattering process, the energy and momentum transfer are $Q'^2 = xQ^2$ and $\nu' = \nu - (1 - x)E$, where E denotes the incident electron energy. For the last term, in the figure, the final-state electron with momentum $p' = xp''$ can be regarded as an equivalent electron, radiated after the electron is scattered off the proton with

$$Q'^2 = (p - p'')^2 = \frac{1}{x} Q^2$$

and

$$\nu' = \nu - \frac{1-x}{x} E' ,$$

where E' is the final-state electron energy. Neglecting the radiative correction to the hadronic system, we have

$$f(\nu, Q^2) \simeq f^{(0)}(\nu, Q^2)[1 + I_e(k, Q^2)]$$

$$+ \int_{1-\Delta E/E}^{1-k/E} dx\, F_e^e(E, x) f^{(0)}(\nu - (1-x)E, xQ^2)$$

$$+ \int_{1-\Delta E/E'}^{1-k/E} dx\, F_e^e\left(\frac{E'}{x'}, x\right)$$

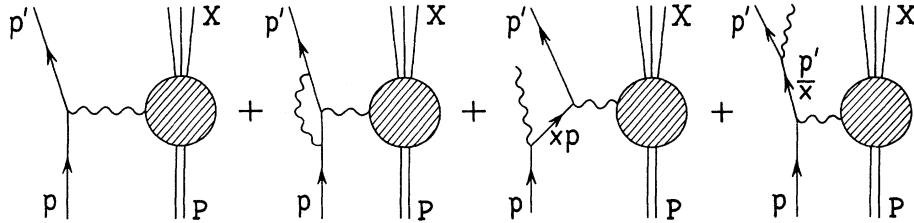$$\times f^{(0)}\left(\nu - \frac{1-x}{x} E', \frac{1}{x} Q^2\right) , \quad (34)$$

where $I_e(k, Q^2)$ is the vertex correction with infrared photon emission (energy smaller than k) included; the leading term of I_e in $\ln Q^2/m_e^2$ is given by[11]

$$I_e(k, Q^2) \simeq -\frac{\alpha}{\pi}\left(\ln\frac{Q^2}{m_e^2} - 1\right)\left(\ln\frac{EE'}{K^2} - \frac{13}{6}\right).$$
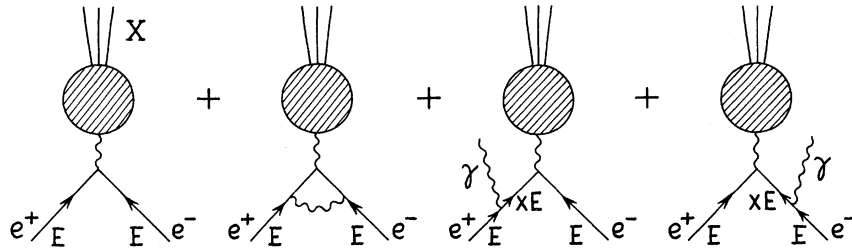
$$(35)$$

ΔE is the energy resolution of the apparatus. The spectrum F_e^e is written up in Fig. 3. For large E and E', Eq. (34) can be expressed in a logarithmically equivalent form in which the previous dependence on the infrared cutoff k is eliminated. Substituting

$$\ln\frac{E}{k} = \int_{1-\Delta E/E}^{1-k/E} \frac{dx}{1-x} + \ln\frac{E}{\Delta E} \quad (36)$$

and taking $\ln E \simeq \ln E'$, Eq. (34) reads

$$f(\nu, Q^2) \simeq f^{(0)}(\nu, Q^2)\left\{1 - \frac{\alpha}{\pi}\left(\ln\frac{Q^2}{m_e^2} - 1\right)\left[\ln\frac{EE'}{(\Delta E)^2} - \frac{13}{6}\right]\right\}$$

$$+ \left\{\frac{2\alpha}{\pi}\ln\frac{E}{m_e}\int_{1-\Delta E/E}^{1}\frac{dx}{1-x}\left[f^{(0)}(\nu - (1-x)E, xQ^2) - f^{(0)}(\nu, Q^2)\right]\right.$$

$$\left. - \frac{\alpha}{\pi}\ln\frac{E}{m_e}\int_{1-\Delta E/E}^{1} dx(1+x)f^{(0)}(\nu - (1-x)E, xQ^2)\right\}$$

$$+ \left\{\frac{2\alpha}{\pi}\ln\frac{E'}{m_e}\int_{1-\Delta E/E'}^{1}\frac{dx}{1-x}\left[f^{(0)}\left(\nu - \frac{1-x}{x}E', \frac{1}{x}Q^2\right) - f^{(0)}(\nu, Q^2)\right]\right.$$

$$\left. - \frac{\alpha}{\pi}\ln\frac{E'}{m_e}\int_{1-\Delta E/E'}^{1} dx(1+x)f^{(0)}\left(\nu - \frac{1-x}{x}E', \frac{1}{x}Q^2\right)\right\} . \quad (37)$$

FIG. 7. (a) Radiative corrections to deep-inelastic electron-proton scattering; (b) radiative corrections to electron-positron annihilation.

In this form, all integrals are separately convergent.

We see that the one-dimensional equivalent-electron approximation (together with the well-known result for the electron vertex correction) provides a simple estimate of the radiative correction. We further use this example to illustrate some limitations of this approximation. First of all, the interference term between the last two terms is neglected. This can be justified insofar as the photons are predominantly emitted along the direction of the parent electron, so the photons emitted from the initial and final electrons will not overlap in the phase space if the relative angle between the two electrons is larger than a few degrees, which is the typical angle for real photon emission. Hence the interference term is negligible for wide-angle scatterings. Secondly, since in the one-dimensional approximation the transverse degrees of freedom relative to the source are averaged over, substantial deviations from Eq. (37) can occur if wide-angle bremsstrahlung of photons is important, as in the case of electron heavy-nucleus scattering. The wide-angle photons, emitted from the initial and final electrons, can have a large probability to overlap in the phase space. Even if the electrons are separated at large angles, the interference term may become important. Thus, in this case, it is better to relinquish equivalent-lepton approximations.

2. Electron-positron annihilation

The one-photon annihilation of e^+e^- into hadrons and its radiative corrections[12] are illustrated in Fig. 7(b). Neglecting the radiative corrections to the hadronic system (which are of minor importance), we have

$$\sigma(Q^2) \simeq \sigma^{(0)}(Q^2)\left[1 + I_e(k, Q^2)\right]$$
$$+ 2\int_{1-\Delta E/E}^{1-k/E} dx\, F_e^e(E, x)\, \sigma_{e^+e^-}^{(0)}(xQ^2) , \quad (38)$$

where E is the incident lepton energy in the e^+e^- c.m. frame, $Q^2 = 4E^2$ is the square of the total energy, and $\sigma_{e^+e^-}^{(0)}$ is the one-photon annihilation cross section. The asymptotic form of the vertex correction[12] I_e is similar to Eq. (35) with $E' = E$, and we can use the same substitution as before to prove that Eq. (38) is independent of the infrared cutoff k:

$$\sigma(Q^2) = \sigma_{e^+e^-}^{(0)}(Q^2)\left[1 - \frac{2\alpha}{\pi}\left(\ln\frac{E}{\Delta E} - \frac{13}{12}\right)\right]$$
$$+ \frac{4\alpha}{\pi}\ln\frac{E}{m_e}\int_{1-\Delta E/E}^{1}\frac{dx}{1-x}\left[\sigma_{e^+e^-}^{(0)}(xQ^2) - \sigma_{e^+e^-}^{(0)}(Q^2)\right]$$
$$- \frac{2\alpha}{\pi}\ln\frac{E}{m_e}\int_{1-\Delta E/E}^{1}dx(1+x)\,\sigma_{e^+e^-}^{(0)}(xQ^2) . \quad (39)$$

For two physically significant cases, the original cross section $\sigma_{e^+e^-}^{(0)}(Q^2)$ can be factored out; if $\sigma_{e^+e^-}^{(0)} = $ const or $\sigma_{e^+e^-}^{(0)} \propto 1/Q^2$, the result can be written as

$$\sigma(Q^2) = \sigma_{e^+e^-}^{(0)}(Q^2)\left[1 - \frac{2\alpha}{\pi}\left(\ln\frac{Q^2}{m_e^2} - 1\right)\left(\ln\frac{E}{\Delta E} - \frac{13}{12}\right)\right.$$
$$\left. + O\left(\frac{\Delta E}{E}\right)\ln\frac{E}{m_e}\right] . \quad (40)$$

The $O(\Delta E/E)$ corrections can easily be calculated if necessary. Another interesting example of Eq. (38) is the radiation tail of a narrow resonance with mass m_R. The cross section $\sigma^{(0)}$ can be approximated by a δ function,

$$\sigma^{(0)}(Q^2) \simeq a\,\delta(Q^2 - m_R^2) . \quad (41)$$

For $Q^2 > m_R^2$, the δ function projects out the distribution function F_e^e in σ:

$$\sigma(Q^2 > m_R^2) = \frac{2a}{Q^2}\frac{\alpha}{\pi}\frac{1 + (m_R^2/Q^2)^2}{1 - m_R^2/Q^2}\ln\frac{E}{m_e} . \quad (42)$$

Just above the resonance, the energy dependence of the cross section is governed by the pole factor $(Q^2 - m_R^2)^{-1}$.

In a similar fashion we can write down the radiative corrections for a wide class of process involving only photon emission from external lepton lines and well-known vertex corrections, but we shall not elaborate further.

IV. MULTISTEP APPLICATIONS

Multistep equivalent-photon and -lepton approximations, as introduced in Refs. 3 and 5, can greatly simplify the calculation of higher-order electromagnetic process. The one-dimensional approach appreciably simplifies the integrations over the phase space. In this section, we present some complex examples to examine the accuracy of this approach.

A. $e^+e^- \to e^+e^-X$ (e^+ and e^- scattered into forward and backward hemispheres)

This process is nothing but a natural extension of inelastic Compton scattering discussed earlier [see Fig. 8(a)]. The positron is merely used as a source of quasireal photons. The cross section has been obtained in Ref. 8 by calculating covariant Feynman diagrams and in Ref. 5 by a two-step equivalent-photon and -lepton approximation. In the latter approach the differential cross section is given by

$$\frac{d\sigma}{dM^2} = \frac{1}{4xE^2}\frac{d\sigma}{dx}$$
$$= \frac{1}{4E^2}\,{}_2F_e^e\left(E, z = \frac{M^2}{4E^2}\right)\sigma_{e^+e^- \to x}(M^2) , \quad (43)$$

where $M^2 = 4xE^2$ is the invariant mass squared of the final-state system X and $_2F_e^e(E, z)$ is the spectrum given in Fig. 5. Thus

$$\frac{d\sigma}{dM^2} \simeq 2\left(\frac{\alpha}{\pi}\right)^2 \frac{\sigma_{e^+e^- \to x}(M^2)}{M^2}\left(\ln\frac{E}{m_e}\right)^2 . \quad (44)$$

The result is identical to the exact calculation in Ref. 8 as long as E and M are logarithmically equivalent. In a more precise procedure, Eq. (44) can be compared with the double differential cross section $d^2\sigma/dM^2 d\cos\theta$ numerically integrated over the entire range of the electron scattering angle θ in the e^+e^- c.m. frame. Agreement is found within 20%. But we want to emphasize that Eq. (42) gives the cross section integrated over all values of θ. Since $d^2\sigma/dM^2 d\cos\theta$ is forwardly peaked and the small-θ region is experimentally impossible to measure, results such as Eq. (44) might overestimate the cross section by a factor of 2 or 3 for experimentally realistic cases (as shown in Ref. 8).

B. $e^+e^- \to e^+e^-\mu^+\mu^-$ (e^+ and e^- scattered into forward hemisphere)

This process is illustrated in Fig. 8(b), and it can again be regarded as a natural extension of $\gamma\gamma^*$ annihilation. Thus, we have

$$d\sigma = 2\int dx\, _2F_e^\mu(E, x)\, d\sigma^{\mu e} , \quad (45)$$

where $_2F_e^\mu(E, x)$ is the equivalent muon spectrum of an electron and $d\sigma^{\mu e}$ is the μe Rutherford cross section for incident muon energy xE. Putting all expressions together, one obtains the final result

$$\frac{d^2\sigma}{d\nu\, dQ^2} = \frac{16\alpha^4}{\pi}\frac{1 - y + y^2/2}{\nu Q^4}\ln\frac{E}{m_e}\ln\frac{E}{m_\mu} , \quad (46)$$

with the variables defined as

$$Q^2 = -[p(e) - p(e')]^2 , \quad (47a)$$

$$\nu = p(e^+)\cdot[p(e) - p(e')] , \quad (47b)$$

$$y = \nu/[p(e)\cdot p(e^+)] . \quad (47c)$$

The accuracy and the kinematical restrictions of Eq. (46) are very similar to those for the previous process, and this discussion should not be repeated here.

C. Trident production[4]

Let us consider the production of a massive muon pair in deep-inelastic electron-proton scattering. As shown in Fig. 8(c) there are three processes contributing to the production cross section in the same order of α. The first two terms are to be regarded as background to the more interesting case where the muon pair emerges out of the hadron system. For very massive muon pairs, the first diagram is the most important background. It can easily be estimated in the equivalent-photon and -lepton approximation because it
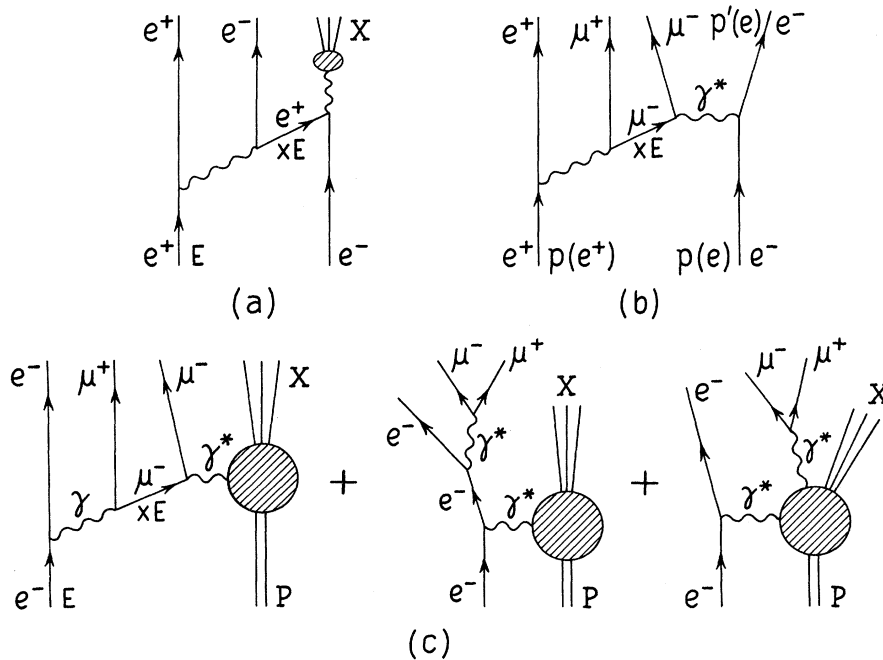

FIG. 8. (a) Double-step electron-positron annihilation; (b) muon pair production in electron-positron scattering; (c) muon pair production in inelastic electron-proton scattering.

can be regarded as (equivalent) muon proton deep-inelastic scattering with the muon spectrum given in Fig. 5. Thus, for the cross section

$$d\sigma = 2 \int dx_2 F_e^\mu(E, x) \, d\sigma^{\mu P} \qquad (48)$$

(where $d\sigma^{\mu P}$ is the μp scattering cross section with incident muon energy xE) we get

$$\frac{d^2\sigma}{dQ^2 \, dm_{\mu\mu}^2} = 4 \left(\frac{\alpha}{\pi} \ln \frac{E}{m_e}\right)^2 \frac{1}{Q^2} \left(\frac{d\sigma^{\mu P}}{dQ_x^2}\right) . \qquad (49)$$

$m_{\mu\mu}^2$ denotes the square of the invariant muon-pair mass, $-Q^2$ is the (squared) momentum transfer from the initial electron to the muon scattered with large angle; $d\sigma^{\mu P}/dQ_x^2$ denotes the inelastic muon-proton differential cross section under the conditions

initial muon energy $E_x = (1 - m_{\mu\mu}^2/Q^2)E$, (50a)

momentum transfer $Q_x^2 = Q^2 - m_{\mu\mu}^2$. (50b)

Notice that the relative energy flux x through the muon lines is given by

$$x = 1 - \frac{m_{\mu\mu}^2}{Q^2} \qquad (51)$$

if momentum transfer Q^2 and invariant mass $m_{\mu\mu}$ are kept fixed.

We conclude this section with a general remark on the applicability of the multistep approximations: The single-step approximation requires $E \gg m_e$. In multistep approximations, this requirement has to be satisfied for the subenergy of each intermediate source. In other words, $xE \gg m_e$ must be fulfilled when this method is applied. All energies involved have to be logarithmically equivalent to E, i.e., they must stay in a finite ratio to each other. If x is integrated over, there may be sizable corrections from the region $x \sim m_e/E$ (the wee region in the parton language).

V. DISCUSSIONS

In this article we have elaborated a simple framework of a one-dimensional equivalent-photon and -lepton approximation. In this approximation the cross section can be regarded as the convolution of one-dimensional photon and lepton distributions with remaining skeleton cross sections. These distributions, the equivalent-photon and -lepton spectra, are simple functions of the scaling variable x (which measures the energy fraction a daughter particle receives from its parent) multiplied with logarithmic energy factors. So, we can estimate high-order QED processes without carrying out tedious Dirac-algebra calculations and watching phase factors. The phase-space integrals are greatly simplified, too. Such advantages are achieved at the cost of limitations described in the previous sections. They can be summarized by the requirement that all energies involved are much larger than the electron mass and that they all stay in a finite ratio to each other (generalized Bjorken limits). Once this requirement is fulfilled in a specific process, the equivalent-particle method provides a powerful means for speedy estimates of high-order QED cross sections in the tree-graph approximation. That has been demonstrated by numerous examples (of practical use) in the preceding sections.

*Work supported in part by the U. S. Atomic Energy Commission.

†Present address.

‡Max Kade Fellow. Present address: III. Physikalisches Institut der Technischen Hochschule, Aachen, W. Germany.

[1]C. F. von Weizsäcker, Z. Phys. **88**, 612 (1934); E. J. Williams, Phys. Rev. **45**, 729 (1934).

[2]P. Kessler, Nuovo Cimento **16**, 809 (1960).

[3]V. N. Baier, V. S. Fadin, and V. A. Khoze, Nucl. Phys. **B65**, 381 (1973).

[4]J. D. Bjorken, J. B. Kogut, and D. E. Soper, Phys. Rev. D **3**, 1382 (1971); S. J. Brodsky, R. Roskies, and R. Suaya, ibid. **8**, 4574 (1973).

[5]N. Cabibbo and M. Rocca, CERN Report No. CERN-TH. 1872 (unpublished).

[6]Angle-dependent formulas have been investigated in Ref. 3.

[7]S. J. Brodsky, in Proceedings of the 1971 International Symposium on Electron and Photon Interactions at High Energies, edited by N. B. Mistry (Laboratory of Nuclear Studies, Cornell University, Ithaca, New York, 1972); P. Kessler, in proceedings of the International Colloquium on Photon-Photon Collisions in Electron-Positron Storage Rings, Collège de France, Paris, 1973 [J. Phys. (Paris) Suppl. **35**, C2-97 (1974)]; H. Terazawa, Rev. Mod. Phys. **45**, 615 (1973).

[8]Min-Shih Chen and P. Zerwas, Phys. Rev. D **11**, 58

(1975).

[9]K. Fujikawa, Nuovo Cimento 12A, 83 (1972).

[10]For a general review, see Y.-S. Tsai, SLAC Report No. SLAC-PUB-1365 (unpublished), and references quoted therein.

[11]Y. S. Tsai, Phys. Rev. 122, 1898 (1961); D. R. Yennie,

S. C. Frautschi, and H. Suura, Ann. Phys. (N.Y.) 13, 379 (1961); L. W. Mo and Y. S. Tsai, Rev. Mod. Phys. 41, 205 (1969).

[12]G. Bonneau and F. Martin, Nucl. Phys. B27, 381 (1971); Y. S. Tsai, Phys. Rev. 120, 269 (1960).